



XXIV Italian Group of Fracture Conference, 1-3 March 2017, Urbino, Italy

## Experimental and numerical investigations of fracture behavior of magnetostrictive materials

M. Colussi<sup>a</sup>, F. Berto<sup>b,\*</sup>, S.M.J. Razavi<sup>b</sup>, M.R. Ayatollahi<sup>c</sup>

<sup>a</sup> Department of Management and Engineering, University of Padua, Stradella S. Nicola 3, Vicenza 36100, Italy.

<sup>b</sup> Department of Mechanical and Industrial Engineering, Norwegian University of Science and Technology (NTNU), Richard Birkelands vei 2b, 7491, Trondheim, Norway.

<sup>c</sup> Department of Mechanical Engineering, Iran University of Science and Technology, Narmak, 16846, Tehran, Iran.

---

### Abstract

The purpose of this work is the characterization of the fracture behaviour of giant magnetostrictive materials subjected to a magnetic field. Both experimental and numerical investigations have been performed, focusing on iron and rare earth alloys, such as the commercially named Terfenol-D. Tests have been carried out on single-edge precracked specimens subjected to three-point bending in the presence of magnetic fields of various intensities and fracture loads have been measured at different loading rates. Recent studies on local stress fields in proximity of crack and notch tips have shown that Strain Energy Density (SED), averaged in a circular control volume which includes a crack tip, could be a robust parameter in the assessment of brittle fracture resistance of several materials. Coupled-field analyses have then been performed on both plane stress and plane strain finite element models and the effect of the magnetic field on fracture resistance of Terfenol-D alloy was predicted in terms of averaged SED. A relationship between the SED's control volume size and the loading rate has also been proposed.

Copyright © 2017 The Authors. Published by Elsevier B.V. This is an open access article under the CC BY-NC-ND license (<http://creativecommons.org/licenses/by-nc-nd/4.0/>).

Peer-review under responsibility of the Scientific Committee of IGF Ex-Co.

**Keywords:** strain energy density; strain energy release rate; smart materials; giant magnetostrictive materials; fracture toughness; magnetic field.

---

---

\* Corresponding author. Tel.: +47-735-93831.

E-mail address: [filippo.berto@ntnu.no](mailto:filippo.berto@ntnu.no)

## 1. Introduction

Magnetostrictive materials exhibit deformation in response to external magnetic fields and magnetization change in response to applied forces. Among giant magnetostrictive materials, the commercially known Terfenol-D ( $\text{Tb}_{0.3}\text{Dy}_{0.7}\text{Fe}_{1.9}$ ) alloy, made out of iron, terbium and dysprosium, has been recording much interest over the years. The remarkable elongation and the high energy density storing capacity at room temperature are advantages which ensure the great Terfenol-D potential in many applications. Such material is employed in automotive industry, in avionics and in robotics, where magnetostriction based sensors and actuators are commonly used. Terfenol-D is also expected to be used in energy harvesting devices as shown by Zhao et al. (2006).

According to Peterson et al. (1989), giant magnetostrictive alloys such as Terfenol-D are very brittle and then susceptible to in-service fracture. Despite defects caused by manufacturing and cracking could have important influence on the material performances, really few works can be found in literature dealing with this topic. It is therefore of interest to grow the mechanical knowledge around defect's sensitivity to magnetostrictive materials. Numerous methods have been proposed by scholars to evaluate the fracture behavior of different materials (Ayatollahi et al. (2015, 2016); Rashidi Moghaddam et al. (in press)). Lazzarin and Zambardi (2001) introduced the averaged Strain Energy Density (SED) criterion to predict brittle failures, which occur without any plastic deformation. The criterion states that brittle fracture failures occur when the strain energy density averaged in a circular control volume, which includes a crack or notch tip, reaches a critical value dependent on the material. Thereafter many researchers worked on this criterion and proved that it could successfully predict brittle and high cycle fatigue failures of precracked, U- or V-notched specimens made out of several materials, including metals and ceramics. Narita et al. (2012) studied the effect of the magnetic field on fracture behavior of Terfenol-D both experimentally and numerically by means of the energy release rate and showed that the fracture resistance, under mode I, is greater in absence of the magnetic field and decreases with the increase of the latter. They also proved that the resistance decrease may be related to the increase of the energy release rate with increasing magnetic fields. Colussi et al. (2016) showed that SED criterion could be extended to the assessment of brittle behavior of giant magnetostrictive materials, under mode I loading condition, and proposed the use of a control volume having radius 0.07 mm. Here, experimental data set on fracture behavior of Terfenol-D specimens under three point bending has been extended and fracture loads were measured in presence and absence of the magnetic field and at different loading rates. By performing coupled-field finite element analyses the effect of the magnetic field and of the loading rate on Terfenol-D brittle failure has been discussed. The capability of the SED criterion to capture these effects has then been analyzed and, for this purpose, a relationship between the radius of the control volume and the loading-rate has also been proposed.

## 2. Analysis

### 2.1. Basic equations of the material

The basic equations for magnetostrictive materials are outlined as follows. Considering a Cartesian coordinate system,  $O-x_1 x_2 x_3$ , the equilibrium equations are given by:

$$\begin{aligned} \sigma_{ji,j} &= 0; \\ \varepsilon_{ijk} H_{k,j} &= 0; \\ B_{i,i} &= 0 \end{aligned} \tag{1}$$

where  $\sigma_{ji}$ ,  $H_i$  and  $B_i$  are respectively the components of the stress tensor, the intensity vector of the magnetic field and the magnetic induction vector, whereas  $\varepsilon_{ijk}$  is the Levi-Civita symbol. A comma followed by an index denotes partial differentiation with respect to the spatial coordinate  $x_i$  and the Einstein's summation convention for repeated tensor indices is applied. The constitutive laws are given as:

$$\begin{aligned} \varepsilon_{ij} &= s_{ijkl}^H \sigma_{kl} + d_{kij} H_k \\ B_i &= d_{ikl} \sigma_{kl} + \mu_{ik}^T H_k \end{aligned} \tag{2}$$

where  $\varepsilon_{ij}$  are the components of the strain tensor and  $s_{ijkl}^H, d_{ikl}, \mu_{ik}^T$  are respectively the magnetic field elastic compliance, the magnetoelastic constants and the magnetic permittivity. Valid symmetry conditions are:

$$\begin{aligned} s_{ijkl}^H &= s_{jikl}^H = s_{ijlk}^H = s_{klij}^H \\ d_{kij} &= d_{kji} \\ \mu_{ij}^T &= \mu_{ji}^T \end{aligned} \tag{3}$$

The relation between the strain tensor and the displacement vector  $u_i$  is:

$$\varepsilon_{ij} = \frac{1}{2}(u_{j,i} + u_{i,j}) \tag{4}$$

The magnetic field intensity, named  $\varphi$  the potential, is written as:

$$H_i = \varphi_{,i} \tag{5}$$

For Terfenol-D, the constitutive relations can be written as:

$$\begin{Bmatrix} \varepsilon_{11} \\ \varepsilon_{22} \\ \varepsilon_{33} \\ 2\varepsilon_{23} \\ 2\varepsilon_{31} \\ 2\varepsilon_{12} \end{Bmatrix} = \begin{bmatrix} s_{11}^H & s_{12}^H & s_{13}^H & 0 & 0 & 0 \\ s_{12}^H & s_{11}^H & s_{13}^H & 0 & 0 & 0 \\ s_{13}^H & s_{13}^H & s_{33}^H & 0 & 0 & 0 \\ 0 & 0 & 0 & s_{44}^H & 0 & 0 \\ 0 & 0 & 0 & 0 & s_{44}^H & 0 \\ 0 & 0 & 0 & 0 & 0 & s_{66}^H \end{bmatrix} \begin{Bmatrix} \sigma_{11} \\ \sigma_{22} \\ \sigma_{33} \\ \sigma_{23} \\ \sigma_{31} \\ \sigma_{12} \end{Bmatrix} + \begin{bmatrix} 0 & 0 & d_{31} \\ 0 & 0 & d_{31} \\ 0 & 0 & d_{33} \\ 0 & d_{15} & 0 \\ d_{15} & 0 & 0 \\ 0 & 0 & 0 \end{bmatrix} \begin{Bmatrix} H_1 \\ H_2 \\ H_3 \end{Bmatrix} \tag{6}$$

$$\begin{Bmatrix} B_1 \\ B_2 \\ B_3 \end{Bmatrix} = \begin{bmatrix} 0 & 0 & 0 & 0 & d_{15} & 0 \\ 0 & 0 & 0 & d_{15} & 0 & 0 \\ d_{31} & d_{31} & d_{33} & 0 & 0 & 0 \end{bmatrix} \begin{Bmatrix} \sigma_{11} \\ \sigma_{22} \\ \sigma_{33} \\ \sigma_{23} \\ \sigma_{31} \\ \sigma_{12} \end{Bmatrix} + \begin{bmatrix} \mu_{11}^T & 0 & 0 \\ 0 & \mu_{11}^T & 0 \\ 0 & 0 & \mu_{33}^T \end{bmatrix} \begin{Bmatrix} H_1 \\ H_2 \\ H_3 \end{Bmatrix} \tag{7}$$

where:

$$\begin{aligned} &\left. \begin{aligned} \sigma_{23} &= \sigma_{32}, \sigma_{31} = \sigma_{13}, \sigma_{12} = \sigma_{21} \\ \varepsilon_{23} &= \varepsilon_{32}, \varepsilon_{31} = \varepsilon_{13}, \varepsilon_{12} = \varepsilon_{21} \end{aligned} \right\} \\ &\left. \begin{aligned} s_{11}^H &= s_{1111}^H = s_{2222}^H, s_{12}^H = s_{1122}^H, s_{13}^H = s_{1133}^H = s_{2233}^H, s_{33}^H = s_{3333}^H \\ s_{44}^H &= 4s_{2323}^H = 4s_{3131}^H, s_{66}^H = 4s_{1212}^H = 2(s_{11}^H - s_{12}^H) \end{aligned} \right\} \\ &d_{15} = 2d_{131} = 2d_{223}, d_{31} = d_{311} = d_{332}, d_{33} = d_{333} \end{aligned}$$

## 2.2. Averaged Strain Energy Density (SED) approach

According to Lazzarin and Zambardi (2001), the brittle failure of a component occurs when the total strain energy,  $\bar{W}$ , averaged in a specific control volume located at a notch or crack tip, reaches the critical value  $W_c$ . In agreement with Beltrami (1885), named  $\sigma_t$  the ultimate tensile strength under elastic stress field conditions and  $E$  the Young's modulus of the material, the critical value of the total strain energy can be determined by the following:

$$W_c = \frac{\sigma_t^2}{2E} \quad (8)$$

The control volume takes different shapes based on the kind of notch. If the notch is represented by a crack, its opening angle is equal to zero and the control volume is a circumference of radius  $R_c$ , centered on the crack tip. Being this the case, the radius  $R_c$  can be evaluated once known the fracture toughness,  $K_{IC}$ , the tensile stress and the Poisson's ratio,  $\nu$ , of the material, by means of the following expression proposed by Yosibash et al. (2004):

$$R_c = \frac{(1+\nu)(5-8\nu)}{4\pi} \left( \frac{K_{IC}}{\sigma_t} \right)^2 \quad (9)$$

The SED averaged in the control volume can be computed directly by means of a finite element analysis.

## 2.3. Finite element model

In order to compute the averaged strain energy density,  $\bar{W}$ , analyses were performed by means of ANSYS R14.5 finite element code, both in plane strain and plane stress conditions depending on the specimens' width. For the purpose, solid models were used to determine which was the most appropriate condition.

As shown by Tiersten (1969), the basic equations for magnetostrictive materials are mathematically equivalent to those of the piezoelectric materials, so four nodes PLANE13 and eight node SOLID5 coupled-field solid elements from ANSYS' library were used, respectively for plane and solid models, and the magnetic field has been introduced by a voltage difference. The coordinate axes  $x = x_1$  and  $z = x_3$  are chosen such that the  $y = x_2$  axis coincides with the thickness direction and such that the easy axis of magnetization is the z-direction. Because of symmetry, only the half of the model was used in the FEA.

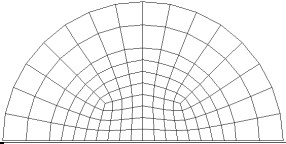
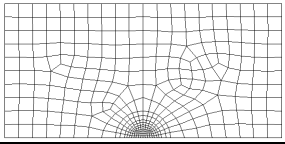
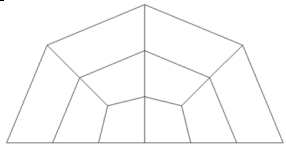
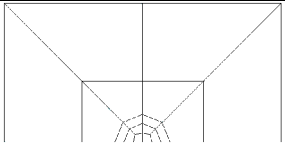
Before carrying out simulations, a mesh sensitivity study was undertaken to determine the adequate finite element (FE) number to be used. SED value have been first determined from a very refined mesh and then from some coarser meshes. The refined mesh had the same FE number adopted in a previous work by the authors, in which finite element models with 6400 elements were used to evaluate the energy release rate by means of J-integral on the same geometry. Among different coarse mesh patterns, it has been found suitable for compute SED without accuracy lost a mesh with 274 elements, of which at 10 elements placed inside the control volume. The results are summarized in Table 1, where the SED value from the proposed coarse mesh is compared with that from the very refined one. The mesh insensitivity is a consequence of the finite element method, in which the elastic strain energy is computed from the nodal displacements, without involving stresses and strains, as shown by Lazzarin et al. (2010).

The relationship between magnetostriction and magnetic field intensity is essentially non-linear. Nonlinearity arises from the movement of the magnetic domain walls, as shown by Wan et al. (2003). To take into account this non-linear behavior, the constants  $d_{15}$ ,  $d_{31}$  and  $d_{33}$  for Terfenol-D, in presence of  $B_z = B_0$ , are given by:

$$\begin{aligned} d_{15} &= d_{15}^m \\ d_{31} &= d_{31}^m + m_{31} H_z \\ d_{33} &= d_{33}^m + m_{33} H_z \end{aligned} \quad (10)$$

Where  $d_{15}^m$ ,  $d_{31}^m$  and  $d_{33}^m$  are the piezomagnetic constants, whereas  $m_{31}$  and  $m_{33}$  are the second order magnetoelastic constants. Jia et al. (2006) proved that if the specimen's dimension in the direction in which the magnetic field is applied is at least two times greater than the other two dimensions, then the longitudinal magnetostriction is prevailing and it can be assumed that only  $d_{33}$  is a function of the magnetic field  $H_z$  and that  $m_{31}$  is equal to zero.

Table 1. Mean values of SED for different mesh refinement.

Number FE (control volume)	Control volume	Control volume	Number FE (model)	$\bar{W}$ [MJ.m <sup>-3</sup> ]	$\Delta\bar{W}$ [%]
128			6400	0.01461	-
10			274	0.01457	-0.3

### 3. Experimental procedure

Among giant magnetostrictive materials, the commercially named Terfenol-D alloy, supplied by Etrema Products, Inc. (USA) was used in all tests and analyses. The material properties are listed in Table 2.

Table 2. Terfenol-D material properties.

Material	Elastic compliance [10 <sup>-12</sup> m <sup>2</sup> .N <sup>-1</sup> ]					Piezo-magnetic constants [10 <sup>-9</sup> mA <sup>-1</sup> ]			Magnetic permeability [10 <sup>-6</sup> Hm <sup>-1</sup> ]		Density [kg.m <sup>-3</sup> ]
	$S_{11}^H$	$S_{33}^H$	$S_{44}^H$	$S_{12}^H$	$S_{13}^H$	$d_{31}^m$	$d_{33}^m$	$d_{15}^m$	$\mu_{41}^T$	$\mu_{33}^T$	$\rho$
Terfenol-D	17.9	17.9	26.3	-5.88	-5.88	-5.3	11	28	6.29	6.29	9250

Test were performed with the aim to measure the fracture load,  $P_c$ , of single edge precracked specimens, subjected to three point bending, in presence and in absence of the magnetic field and at various loading-rates. Specimens were 5 mm thick, 3 mm wide and 15 mm long. Before testing, all specimens were weakened on one side by a 0.5 mm deep crack, which was introduced using a tungsten cutter. Tested specimen is showed in Fig. 1.

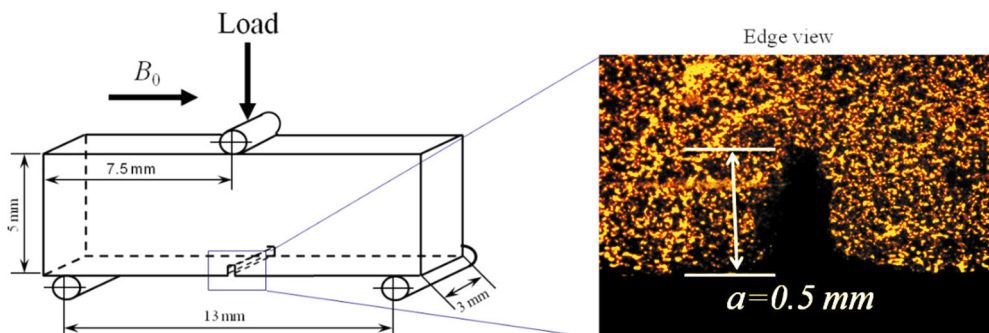


Fig. 1. Specimen's geometry and edge micrograph of the introduced crack.

The load  $P$  has been impressed at the midpoint of the specimens, which were simply supported with span of 13 mm, by means of a 250 N load cell (resolution: 0.01 N). The load was applied for different loading-rates: 0.05, 0.5 and 3.0  $\text{Ns}^{-1}$ . A uniform magnetic field, with magnetic induction  $B_0$ , has been applied in the longitudinal direction through an electromagnet. As devices in which Terfenol-D is employed commonly work in magnetic induction range which varies from 0.02 T to 0.05 T, the representative value of 0.03 T has been adopted in all tests. It is due to point out that, as alloying elements in Terfenol-D are Terbio and Disprosio, which are very expensive rare earths, the number of tested specimens was limited: from two to three at each condition.

By means of experimental procedure it has also been possible to assess the second order magnetoelastic constant,  $m_{33}$ . Let consider a Cartesian coordinate system,  $O-x y z$ , which origin is located at the top center of an uncracked specimen. Varying the intensity of the magnetic field applied in the  $z$ -direction (longitudinal direction), the trend of magnetostriction has been measured through a strain gauge located at  $x = y = z = 0$  mm. By comparison between the measured strain  $\varepsilon_{zz}$  and the numerically obtained one, it has been found that the proper value for the second order magnetoelastic constant is  $4.82 \times 10^{-12} \text{ m}^2 \text{ A}^{-2}$ . This value has been used in the analyses to compute the SED.

#### 4. Results and discussion

Fracture load,  $P_c$ , in presence and absence of the magnetic field have been experimentally measured at each loading-rate. Data, in terms of fracture load, are summarized in Table 3. Bold numbers represent the average value at each condition, whereas numbers in brackets represent the relative standard deviations.

Table 3. measured fracture loads as a function of the loading-rate and the magnetic field.

$dP/dt$	$P_c$ [N]	
	$B = 0$ T	$B = 0.03$ T
0.05 $\text{Ns}^{-1}$	58.3	59.2
	65.8	61.9
	74.7	64.6
	<b>66.3</b> (5.81)	<b>61.9</b> (1.91)
0.5 $\text{Ns}^{-1}$	66.6	60.7
	68.5	61.6
	<b>67.5</b> (0.78)	<b>61.1</b> (0.37)
3.0 $\text{Ns}^{-1}$	71.0	74.2
	79.2	59.3
	-	60.0
	<b>75.1</b> (3.35)	<b>64.5</b> (5.95)

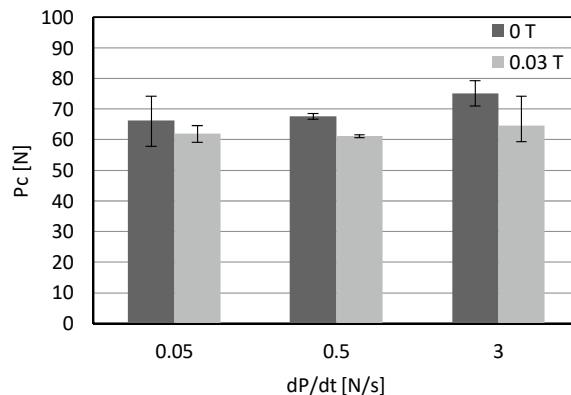


Fig. 2. Mean fracture loads as a function of the loading-rate and the magnetic field

Average fracture loads are presented in Fig. 2. The error bars indicate the maximum and minimum values of  $P_c$ . The average fracture load at  $0.05 \text{ N s}^{-1}$ ,  $0.50 \text{ N s}^{-1}$  and  $3.0 \text{ N s}^{-1}$  are decreased respectively about 7%, 9% and 14% in the presence of the magnetic field. It has also been found that Terfenol-D shows a decrease in fracture load as the loading-rate decreases. Similar behavior has been observed for other materials such as TiAl alloys, by Cao et al. (2007) and piezoelectric ceramics, by Shindo et al. (2009, 2010) and Narita et al. (2012).

To take into account the effect of the loading-rate on Terfenol-D fracture load, here it is assumed that the critical radius  $R_c$ , which depends on the material and on the notch opening angle, varies also with the speed at which the load is applied. By plotting the averaged SED related to the mean values of critical loads in Table 3, in presence and in absence of the magnetic field, as a function of control volume radius, it is possible to determine different intersections for each loading-rate. The intersections have been found at 0.05, 0.056 and 0.1 mm respectively for the loading-rates 0.05, 0.5 and  $3.0 \text{ N s}^{-1}$ . This means that, at the critical load, the material is characterized by a value of strain energy density, averaged in a control volume having size variable with the loading-rate, which is independent of the ratio between the applied load and magnetic field. A good fit of  $R_c$  versus loading-rate to a linear model has been found, then, adopting a simple linear regression model, the following relationship is proposed:

$$R_c = 0.0195 \frac{dP}{dt} + 0.05 \quad (11)$$

The approximated critical radius of 0.07 mm, obtained from (9) and suggested by Colussi et al. (2016) without taking into account the loading-rate, falls amid of the range of variation here proposed.

Fig. 3 shows a summary of the experimental data in terms of the square root of the ratio between the averaged strain energy density,  $\bar{W}$ , and the critical value of strain energy,  $W_c$ . This parameter has been chosen because of its proportionality to the fracture load. The averaged strain energy density,  $\bar{W}$ , has been computed in control volumes having radius given by (11), whereas a critical strain energy equal to  $0.02 \text{ MJ.m}^{-3}$  is assumed. This critical value is obtained from equation (8), assuming Young's modulus equal to 30 GPa, Poisson's ratio equal to 0.25 and tensile strength equal to 34 MPa, which are the medium characteristics provided by the material supplier. Here, Young's modulus is assumed independent from the applied magnetic field. This assumption is reasonable in the range of variation of the applied magnetic field. In Fig. 3 experimental data from Narita et al. (2012) have also been summarized. Data referred to fracture loads measured under three point bending, with and without magnetic a 0.03 T magnetic field, at the following loading-rate:  $0.2 \text{ N s}^{-1}$  and  $3.0 \text{ N s}^{-1}$ . Specimens were 3 mm thick, 5 mm wide and 15 mm long. Crack depth was 0.5 mm. Due to the different geometry (ratio between width and thickness equal to 5/3 instead of 3/5) plane strain condition instead of plane stress condition resulted more appropriate for their modeling. It has been found that about all experimental data fit in a narrow scatter band, which limits are drawn here with an engineering judgment from 0.80 to 1.20 (4 data over 35 being outside of this range). The few data which exceed the band fall however in the safety region of the plot. The averaged SED criterion appears suitable for fracture strength assessment of cracked specimens made out of Terfenol-D alloy, under mode I condition, in presence or absence of the magnetic field and with variable loading-rate. In the authors' opinion the result is satisfactory and the SED criterion permits the reliable assessment of Terfenol-D brittle failure by means of coarse mesh based finite element models. The proposed relationship between the size of the control volume and the loading-rate also permit to take into account the loading-rate by means of static analyses.

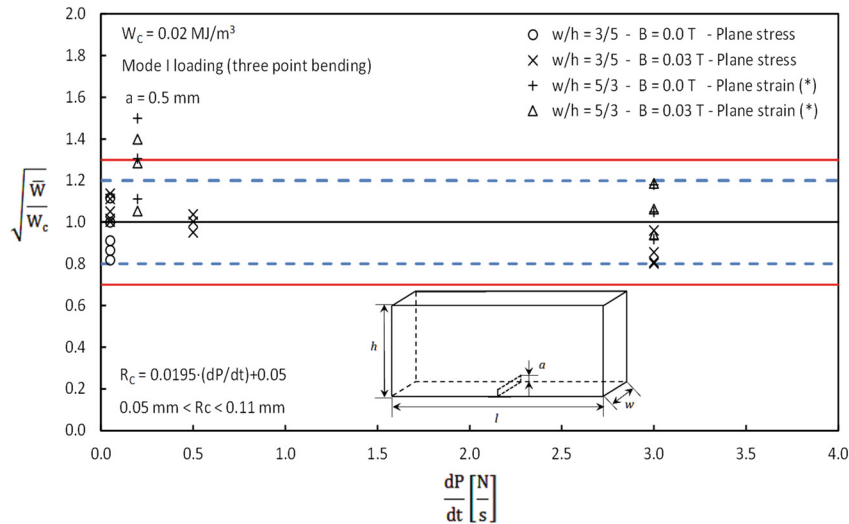


Fig. 3. synthesis from specimens made out of Terfenol-D at various loading-rate in presence and absence of the magnetic field B.

## Conclusions

A combined experimental and numerical study was conducted to understand the defect sensitivity of giant magnetostrictive materials. Under mode I loading condition, it has been found that Terfenol-D shows a decrease in fracture load in presence of a magnetic field. This behavior is justified by the increase of the strain energy with increasing magnetic fields. Terfenol-D also shows a decrease in fracture loads as the loading-rate decreases. Results indicate that SED criterion is able to capture this behavior if a linear relationship between the size of the control volume and the loading-rate is assumed. A good match between experimental results and numerical predictions has been found and a substantial mesh insensitivity of SED approach has been proved.

## References

- Ayatollahi, M.R., Razavi, S.M.J., Rashidi Moghaddam, M., Berto, F., 2015. Mode I fracture analysis of Polymethylmethacrylate using modified energy—based models. *Physical Mesomechanics* 18(5), 53-62.
- Ayatollahi, M.R., Rashidi Moghaddam, M., Razavi, S.M.J., Berto, F., 2016. Geometry effects on fracture trajectory of PMMA samples under pure mode-I loading. *Engineering Fracture Mechanics* 163, 449–461.
- Beltrami, E., 1885. Sulle condizioni di resistenza dei corpi elastici. *Rendiconti del Regio Istituto Lombardo XVIII*, 704–714.
- Berto, F., Lazzarin, P., 2014. Recent developments in brittle and quasi-brittle failure assessment of engineering materials by means of local approaches. *Materials Science and Engineering R* 75, 1–48.
- Berto, F., Lazzarin, P., 2009. A review of the volume-based strain energy density approach applied to V-notches and welded structures. *Theoretical and Applied Fracture Mechanics* 52, 183–194.
- Calkins, F., Flatau, a. b., Dapino, M.J., 2007. Overview of Magnetostrictive Sensor Technology. *Journal of Intelligent Material Systems and Structures* 18, 1057–1066.
- Cao, R., Lei, M.X., Chen, J.H., Zhang, J., 2007. Effects of loading rate on damage and fracture behavior of TiAl alloys. *Materials Science and Engineering: A* 465, 183–193.
- Engdahl, G., 1999. *Handbook of Giant Magnetostrictive Materials*. Academic Press, New York.
- Jia, Z., Liu, W., Zhang, Y., Wang, F., G.D., 2006. A nonlinear magnetomechanical coupling model of giant magnetostrictive thin films at low magnetic fields. *Sensors and Actuators A* 128, 158–164.
- Lazzarin, P., Berto, F., Zappalorto, M., 2010. Rapid calculations of notch stress intensity factors based on averaged strain energy density from coarse meshes: theoretical bases and applications. *International Journal of Fatigue* 32, 1559–1567.
- Lazzarin, P., Zambardi, R., 2001. A finite-volume-energy based approach to predict the static and fatigue behavior of components with sharp V-shaped notches. *International J of Fracture* 112, 275–298.
- Li, P., Wen, Y., Liu, P., Li, X., Jia, C., 2010. A magnetoelectric energy harvester and management circuit for wireless sensor network. *Sensors and Actuators, A: Physical* 157, 100–106.
- Mori, K., Horibe, T., Ishikawa, S., Shindo, Y., Narita, F., 2015. Characteristics of vibration energy harvesting using giant magnetostrictive cantilevers with resonant tuning. *Smart Materials and Structures* 24, 125032.



- Narita, F., Morikawa, Y., Shindo, Y., Sato, M., 2012. Dynamic fatigue behavior of cracked piezoelectric ceramics in three-point bending under AC electric fields. *Journal of the European Ceramic Society* 32, 3759–3766.
- Peterson, D.T., Verhoeven, J.D., McMasters, O.D., Spitzig, W.A., 1989. Strength of Terfenol-D. *Journal of Applied Physics* 65, 3712.
- Rashidi Moghaddam, M., Ayatollahi, M.R., Razavi, S.M.J., Berto, F., (in press). Mode II Brittle Fracture Assessment Using an Energy Based Criterion. *Physical Mesomechanics*.
- Sabir, M., Maugin, G.A., 1996. On the fracture of paramagnets and soft ferromagnets. *International Journal of Non-Linear Mechanics* 31, 425–440.
- Shindo, Y., Mori, K., Narita, F., 2010. Electromagneto-mechanical fields of giant magnetostrictive / piezoelectric laminates. *Acta Mechanica* 212, 253–261.
- Shindo, Y., Narita, F., Mori, K., Nakamura, T., 2009. Nonlinear bending response of giant magnetostrictive laminated actuators in magnetic fields. *Journal of Mechanics of Materials and Structures* 4, 941–949.
- Tiersten, H.F., 1969. *Linear piezoelectric plate vibrations: elements of the linear theory of piezoelectricity and the vibrations of piezoelectric plates*. Springer, New York.
- Wan, Y., Fang, D., Hwang, K.C., 2003. Non-linear constitutive relations for magnetostrictive materials. *International Journal of Non-Linear Mechanics* 38, 1053–1065.
- Yosibash Z., Bussiba A. R., G.I., 2004. Failure criteria for brittle elastic materials. *International Journal of Fracture* 125, 307–333.
- Zhao, X., Lord, D.G., 2006. Application of the Villari effect to electric power harvesting. *Journal of Applied Physics* 99, 08M703.